The Journal of Neuroscience, June 1992, 12(6): 2104–2111

# Differential Properties of Tetrodotoxin-sensitive and Tetrodotoxin-resistant Sodium Channels in Rat Dorsal Root Ganglion Neurons

**Mary Louise Roy and Toshio Narahashi**

Department of Pharmacology, Northwestern University Medical School, Chicago, Illinois 60611

**TTX-sensitive (TTX-S) and TTX-resistant (TTX-R) sodium channel currents were analyzed in acutely dissociated dorsal root ganglion (DRG) neurons isolated from 3–12-d-old and adult rats. Currents were recorded using the whole-cell patch-clamp technique. TTX-R current was more likely to be present in younger animals (3–7 d), whereas TTX-S current was more common in older animals (7–10 d), although TTX-R current was recorded from adult rat DRG neurons. The TTX-R and TTX-S currents differed in their steady-state inactivation, with 50% inactivation voltage at $-40 \pm 5$ mV ($n = 10$) for TTX-R currents and $-70 \pm 4$ mV ($n = 10$) for TTX-S currents. These current types also differed in their activation kinetics, with 50% activation values of $-15 \pm 5$ mV ($n = 5$) for TTX-R currents and $-26 \pm 6$ mV ($n = 5$) for TTX-S currents. The interactions of TTX-R and TTX-S channels with various pharmacological agents and divalent cations were studied. The $K_d$ values for TTX-S and TTX-R currents were estimated to be 0.3 nM and 100 μM for TTX, 0.5 nM and 10 μM for saxitoxin, and 50 μM and 200 μM for lidocaine, respectively. TTX-S channels did not exhibit a marked use-dependent block by lidocaine, whereas lidocaine significantly decreased TTX-R current in a use-dependent manner at frequencies ranging from 1 to 33.3 Hz. Several external divalent cations exerted different effects on these current types. Addition of 5 mM $Ca^{2+}$ reduced TTX-S current 22 ± 3.1% ($n = 5$) and TTX-R current 8.2 ± 3% ($n = 5$). Addition of 50 μM $Pb^{2+}$ reduced TTX-S current 20.6 ± 2.2% ($n = 5$) and TTX-R current 70.4 ± 5.1% ($n = 5$), whereas 5 mM $Cd^{2+}$ reduced TTX-S current 30.1 ± 4.0% ($n = 5$) and TTX-R current 85.3 ± 4.2% ($n = 5$). $Pb^{2+}$ and $Cd^{2+}$, but not $Ca^{2+}$, exerted significant depolarizing shifts in the conductance–voltage relationships of TTX-R and TTX-S currents. The biophysical and pharmacological properties of these two types of sodium channels are of particular importance in the development of the CNS and in the mechanism of action of drugs on the CNS neurons.**

Tetrodotoxin (TTX), a toxin contained in the ovaries and liver of pufferfish, has proven to be a useful tool in the electrophysiological and molecular study of ion channels (Narahashi, 1974, 1988). Sodium channel currents in various neuronal preparations are selectively and reversibly blocked by externally applied TTX, with nanomolar $K_d$ values in a one-to-one stoichiometric relationship. TTX block does not alter the sodium channel gating current and the kinetics of sodium current.

In addition to these TTX-sensitive (TTX-S) sodium channels, TTX-resistant (TTX-R) sodium channels with micromolar $K_d$ values have been found in neuronal, denervated skeletal muscle, and cardiac muscle preparations. In the latter two tissues, the primary structures of TTX-R channels are virtually identical (Rogart et al., 1989; Kallen et al., 1990). Neuronal TTX-R channels have been reported in sensory neurons of bullfrog (Campbell, 1988; Guo and Strichartz, 1990) and garter snake (Jones, 1986), group C sensory neurons (Bossu and Feltz, 1984), and nodose neurons (Ikeda et al., 1986; Ikeda and Schofield, 1987) in rat, and dorsal root ganglion (DRG) neurons in human (McLean et al., 1988) and mouse (Matsuda et al., 1978; Yoshida et al., 1978).

Electrophysiological analysis of TTX-R and TTX-S channels in rat DRG neurons was first reported by Kostyuk et al. (1981). The work of Kostyuk et al., and that of others, indicates that these channels differ in their activation and inactivation kinetics (Roy and Narahashi, 1990; Schwartz et al., 1990) and their interactions with externally applied divalent cations (Roy and Narahashi, 1991). Developmental expression of these channels has also been reported (Roy and Narahashi, 1990; Schwartz et al., 1990), as well as modulation of current expression by NGF (Omri and Meiri, 1990).

The present study characterizes the electrophysiological properties of TTX-R and TTX-S sodium channel currents in acutely dissociated rat DRG neurons, and examines the interactions of TTX, saxitoxin (STX), divalent cations, and lidocaine with these channels. It was found that each of these agents exerted differential effects on TTX-R and TTX-S channels in this preparation.

## Materials and Methods

*Dorsal root ganglion neuron preparations.* Neurons were acutely dissociated from rat dorsal root ganglia and maintained in a short-term primary culture to be used within a 24 hr period. A 3–12-d-old or adult Sprague–Dawley rat was anesthetized with sodium pentobarbital (i.p., 0.4 ml at 3 mg/ml). The vertebral column was then removed and cut longitudinally, generating two hemisections, which were placed into sterile $Ca^{2+}$- and $Mg^{2+}$-free phosphate-buffered saline solution (PBS). The ganglia were isolated from the spinal lumen and enzymatically treated to weaken the encapsulating tissue around the neuronal cell bodies with PBS containing either a mixture of cysteine (0.5 mg/ml), papain (0.8 mg/ml), and collagenase-dispase (0.2 mg/ml), or trypsin alone (2.0 mg/ml). Both procedures required incubation at 36°C for approximately 20 min. The cells were then rinsed twice with culture

Received Sept. 3, 1991; revised Dec. 26, 1991; accepted Dec. 30, 1991.

This work was supported by NIH Grants R01 NS14143 (T.N.) and F31 MH09839 (M.L.R.). We thank Mr. J. Bloom for his technical support, and Ms. Vicky James-Houff for her secretarial assistance.

Correspondence should be addressed to Dr. Toshio Narahashi, Department of Pharmacology, Northwestern University Medical School, 303 East Chicago Avenue, Chicago, IL 60611.

media (serum-free Dulbecco's Modified Eagle's Medium) containing gentamycin (0.08 mg/ml). Using a sterile Pasteur pipette, neurons were mechanically isolated from extraneous tissue by trituration. The resulting cloudy cell suspension was evenly dispersed into cluster dish wells, with each well containing a 12 mm polylysine-coated glass coverslip and 1.0 ml of culture medium. Generally, 1 or 2 hr of incubation (5–10% $CO_2$, 100% humidity) were necessary to allow cells to settle and adhere to the coverslips.

*Electrical recording.* One coverslip supporting cells was transferred to a 1.5 ml glass-bottomed Plexiglas perfusion chamber on the stage of a Swift inverted microscope. A whole-cell configuration of the patch-clamp technique (Hamill et al., 1981) was used to record membrane currents. Borosilicate glass capillary tubes were pulled to make suction pipettes with resistances of 0.75–2 MΩ. Inverted voltage-clamp command pulses were applied to the bath through an Ag–AgCl pellet/3 M KCl–agar bridge. The membrane currents thus generated were recorded by a current-to-voltage converter consisting of an operational amplifier and a 10 MΩ feedback resistor. Data were stored on hard and floppy disk drives using a PDP 11/73 Digital computer.

The liquid junction potential between internal and external solutions was approximately −5 mV, and all data were compensated for this value. The series resistance of the recording system was compensated by the addition of a small portion of the current–voltage convertor output voltage to the command pulse. This was done by speeding up the decay of the capacitive transient current (Marty and Neher, 1983; Matteson and Armstrong, 1984). Leakage and capacitive currents were digitally subtracted with $P - P/4$ procedures (Benzanilla and Armstrong, 1977).

*Solutions.* External and internal solutions were designed to separate sodium channel currents from other channel currents. The external solution contained (in mM) NaCl, 75; $MgCl_2$, 1; $CaCl_2$, 1.8; KCl, 5; glucose, 55; *N*-2-hydroxyethylpiperazine-*N*-2-ethanesulfonic acid (HEPES), 5.5; Na-HEPES, 4.5; and tetramethylammonium chloride, 40; with a final pH of 7.4. The intracellular solution contained (in mM) CsF, 110; NaF, 10; CsCl, 30; $MgCl_2$, 2; ethylene glycol bis-(β-aminoethylether)-*N,N,N′,N′*-tetraacetic acid (EGTA), 2; HEPES, 10; and calpain inhibitor II (Calbiochem, St. Louis, MO), 0.2; with the pH adjusted to 7.3 with 1 M NaOH. The osmolarity of each solution was adjusted to 300 mOsm with glucose. External solutions were applied to the chamber via a gravity perfusion system and cooled with a Peltier device to 13–18°C. The temperature did not fluctuate more than 1°C during the course of an experiment.

TTX was dissolved in 2.0 mM citric acid to make 100 mM stock solution, which was kept frozen until use. It was diluted with the external solution to give the desired final TTX concentrations (0.1 nM to 100 μM). STX stock solution was similarly stored and diluted with the external solution. Lidocaine hydrochloride was dissolved in 0.1 M HCl to make 0.1 M stock solution.

## Results

### *Developmental expression patterns of TTX-R and TTX-S channel currents*

The sodium current recorded from each neuron consisted of TTX-R and TTX-S channel currents in various proportions that correlated to animal age (Fig. 1) and cell size. Acute dissociations of DRGs from younger animals (3–4 d) yielded a large number of small cells (≤15 μm) that expressed solely or mainly TTX-R current. Cells from animals 4–8 d of age were of comparable size but tended to express mixtures of TTX-R and TTX-S currents. Preparations from older animals (8–12 d) and adults had a greater number of larger cells (≥20 μm) that exhibited solely or mainly TTX-S current as well as a minor population of the small-diameter cells expressing TTX-R current. While these correlations were seen during most experiments, occasional exceptions were found.

### *TTX-S and TTX-R currents*

TTX-S and TTX-R currents showed strikingly different time courses of both activation and inactivation. Examples of the two types of currents recorded from two cells, one expressing

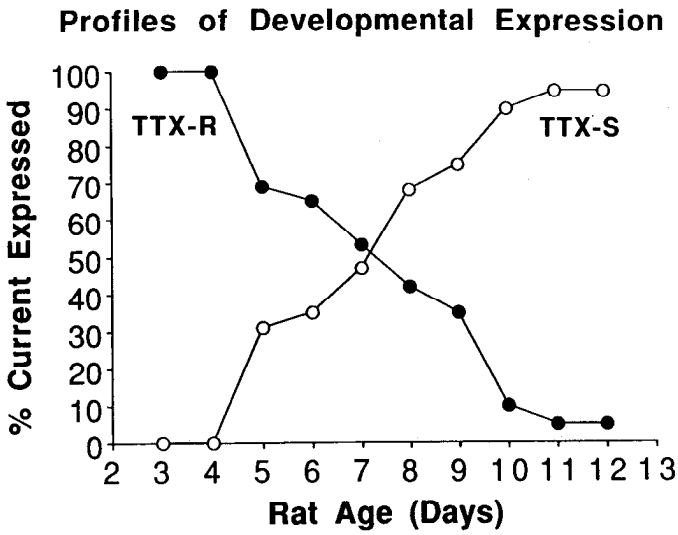


*Figure 1.* Profiles of TTX-R and TTX-S current expression plotted as a function of rat age. Cells isolated from younger (3–4 d) and older (10–12 d and adult) animals were found to express a majority of TTX-R and TTX-S currents, respectively. Preparations from 5–9-d-old animals expressed a mixture of current types, with the percentage of TTX-R current decreasing with age. Values for TTX-R and TTX-S current expression were based upon the ratio of current blocked (TTX-S) or unaffected (TTX-R) by 100 nM TTX to total current (day 3, $n = 5$; day 4, $n = 5$; day 5, $n = 19$; day 6, $n = 33$; day 7, $n = 38$; day 8, $n = 29$; day 9, $n = 10$; day 10, $n = 10$; days 12+, $n = 4$).

TTX-S current and the other expressing TTX-R current, are shown in Figure 2, *A* and *B*. The cells were depolarized in +10 mV steps from a holding potential of −80 mV to +70 mV, and the resulting currents were recorded. TTX-S current exhibited much faster time courses of activation and inactivation than TTX-R current. Indeed, at the end of the 40 msec test pulse, less than 10% of TTX-S current remained, whereas ~50% of the TTX-R current was still activated.

The amplitude of peak current recorded from a cell expressing both TTX-S and TTX-R currents is plotted as a function of test voltage in Figure 2*C*. Total current, as well as the TTX-R current measured in the presence of 10 μM TTX, is shown. Also plotted is the TTX-S component obtained by subtraction of TTX-R current from total current. The reversal potentials of +38 to +40 mV are in close agreement with the calculated $E_{Na}$ of +39.96 mV for this experiment, with 50 mM external sodium. As expected, both TTX-R and TTX-S currents had the same reversal potential, and removal of external sodium ions effectively eliminated both TTX-R and TTX-S currents (not shown).

### *Steady-state sodium channel inactivation*

TTX-R and TTX-S sodium channel currents exhibited markedly different voltage dependence of their inactivation. Figure 3 shows the steady-state inactivation profile of a cell expressing both TTX-R and TTX-S currents. Measurements were made by using a standard two-pulse protocol. A 1.0 sec conditioning pulse to various potential levels was followed by, with a 0.7 msec interpulse interval, a 40 msec test pulse to +10 mV (Fig. 3, *A–C*, inset). The 0.7 msec interpulse interval was used to allow the capacitive transient current to decay prior to the onset of the test pulse. The peak current amplitudes recorded during the test pulse were normalized to their maximum value and are plotted against prepulse voltage levels (Fig. 3*D*). TTX-S and

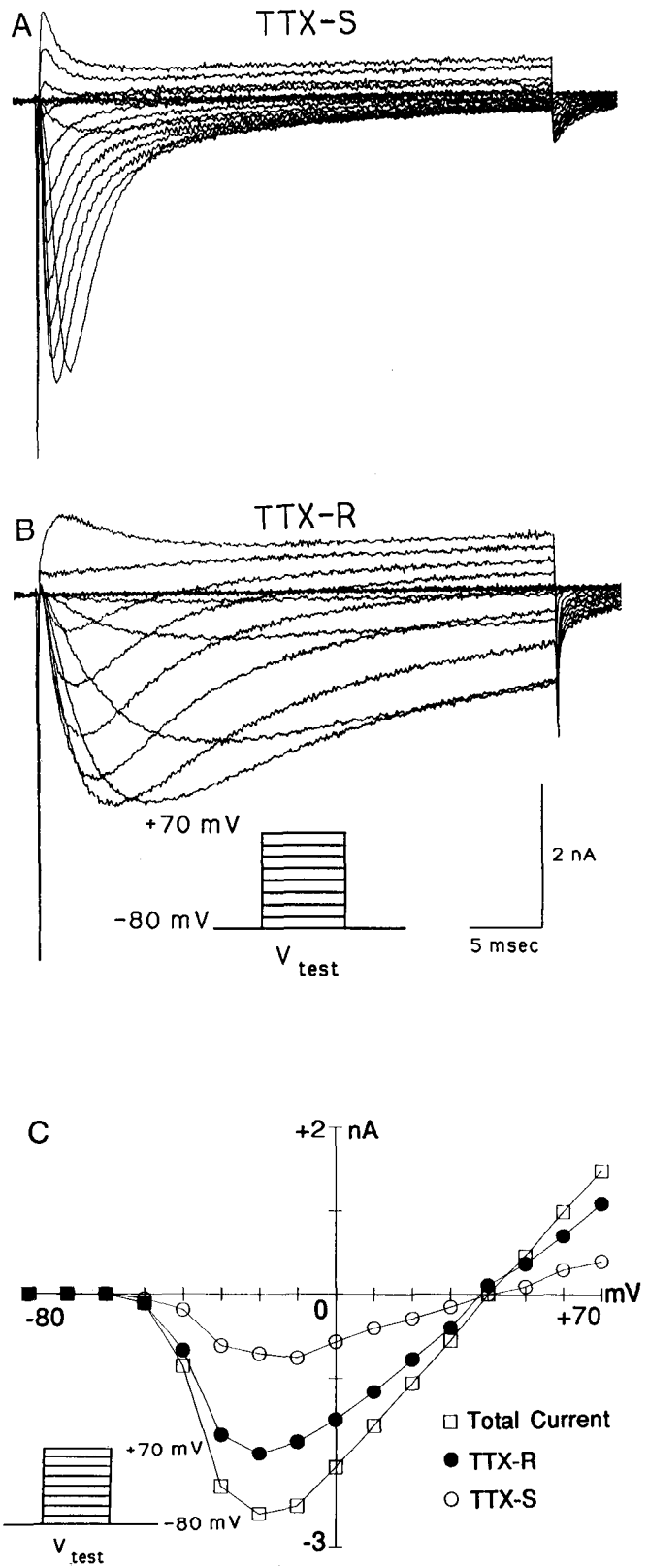


*Figure 2.* Families of TTX-S and TTX-R currents and current–voltage relationships. *A*, TTX-S currents recorded during 40 msec test pulses using the pulse protocol indicated in the *inset* of *B*. This neuron was isolated from an 8-d-old rat. Note the rapid onset and decay of current. *B*, TTX-R currents generated using the pulse protocol indicated in the *inset*. This neuron was isolated from a 3-d-old rat. Note the markedly slower current onset and decay relative to the TTX-S current in *A*. *C*, Peak current amplitude as plotted as a function of membrane potential. Pulse protocol is shown in the *inset*. This cell was isolated from a 6-d-old rat, expressing both TTX-S and TTX-R currents. Currents were first recorded in the absence of TTX (total current, *open squares*), and then in the presence of 10 μM TTX (TTX-R current, *solid circles*). TTX-R values were subtracted from those of total current, and the resultant TTX-S current (*open circles*) was plotted. Note that both types of channels show the same reversal potential.

TTX-R currents exhibited half-maximal inactivation values at $-70 \pm 4$ mV ($n = 10$) and $-40 \pm 5$ mV ($n = 10$) (mean ± SEM), respectively.

*Kinetics of sodium channel activation*

In addition to their different steady-state inactivation profiles, TTX-S and TTX-R currents had distinct activation kinetics. Cells exhibiting only TTX-R or TTX-S currents were subjected to a protocol to measure current–voltage relationships. Depolarizing pulses of 40 msec duration were applied from a holding potential of −80 mV with 10 mV increments at 20 msec intervals. From the peak amplitude of sodium current ($I_{Na}$) thus measured, the sodium conductance ($G_{Na}$) was calculated from the equation $G_{Na} = I_{Na}/(E - E_{Na})$, where $E$ is the membrane potential and $E_{Na}$ is the reversal potential for sodium. The sodium conductance is plotted as a function of the membrane potential in Figure 4. Values for 50% activation are estimated to be $-26 \pm 6$ mV ($n = 5$) for TTX-S currents and $-15 \pm 5$ mV ($n = 5$) for TTX-R currents.

At 13–18°C, TTX-R current had a slow time course, with a time-to-peak current at 5–10 msec (Figs. 2*B*, 3*B*), whereas TTX-S current had a fast time course with a short (<5 msec) time-to-peak current (Figs. 2*A*, 3*C*).

*Dose–response curves for tetrodotoxin and saxitoxin*

The affinities of TTX-R and TTX-S channels for TTX and STX are strikingly similar (Fig. 5*A,B*). Cells expressing only TTX-S ($n = 3$) or TTX-R ($n = 3$) currents were exposed to various concentrations of each toxin, with test pulses (one per minute) to +10 mV from a holding potential of −80 mV. The amplitude of peak current in test solutions was normalized to that of control current and is plotted against toxin concentration. The $K_d$ values for TTX-S and TTX-R currents were estimated to be 0.3 nM and 100 μM for TTX and 0.5 nM and 10 μM for STX, respectively. Block of TTX-S current by both toxins was reversible following 20–40 min of wash with toxin-free solution. However, block of TTX-R current by either toxin was reversed more easily despite higher toxin concentrations used, requiring only 2–5 min of wash.

*Dose–response curves for lidocaine and use-dependent block*

Whereas TTX and STX are believed to share a common extracellular binding site on the sodium channel (Hille, 1975), local anesthetics block the channel primarily from inside of the membrane (Frazier et al., 1970; Narahashi et al., 1970). The dose–response curves for lidocaine block of TTX-R and TTX-S currents were analyzed using the same pulse protocol as that for TTX and STX, with test pulses applied once every minute to avoid use-dependent block. The amplitudes of normalized peak currents of cells expressing only TTX-S ($n = 3$) or TTX-R ($n = 3$) currents are plotted against lidocaine concentrations in Figure 6*A*. The $K_d$ values were estimated to be 50 μM and 200 μM for TTX-S and TTX-R currents, respectively.

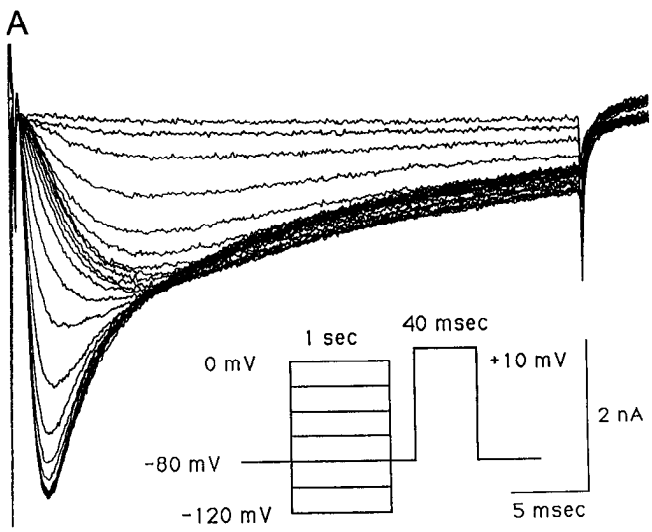


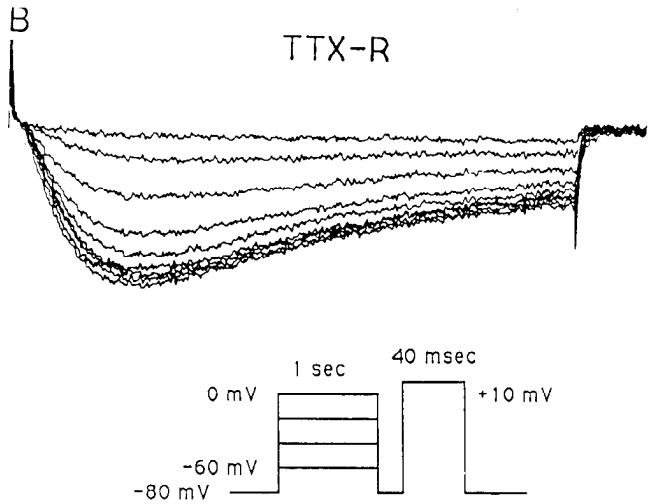


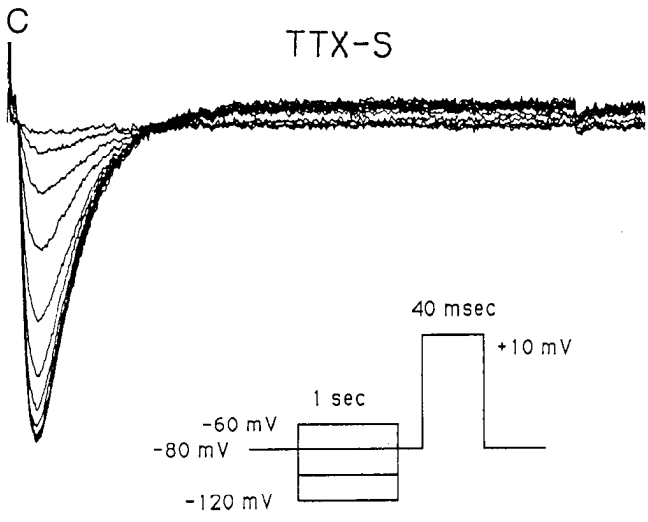


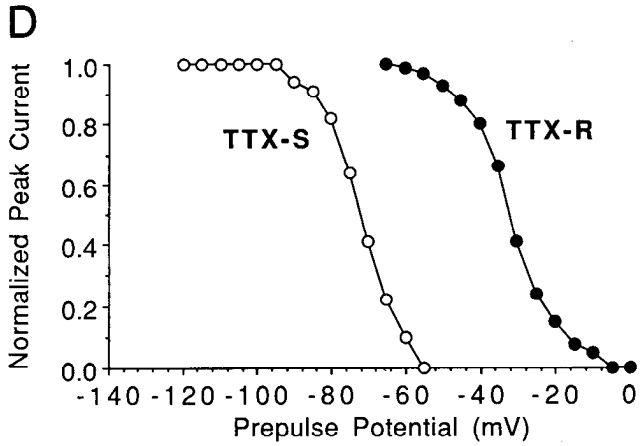


*Figure 3.* Steady-state sodium channel inactivation profiles. *A,* Total sodium currents evoked from a single cell expressing both TTX-R and TTX-S channels. *B,* TTX-R currents plotted separately; they are virtually identical to data seen in the presence of 10 $\mu$M TTX. *C,* TTX-S currents isolated by subtraction of TTX-R current observed after a prepulse of −60 mV. Pulse protocols corresponding to current records are indicated in the *insets* in *A–C. D,* Normalized peak current versus prepulse amplitude. For this cell, 50% inactivation voltages for TTX-S and TTX-R currents were −72.5 mV and −35.4 mV, respectively.

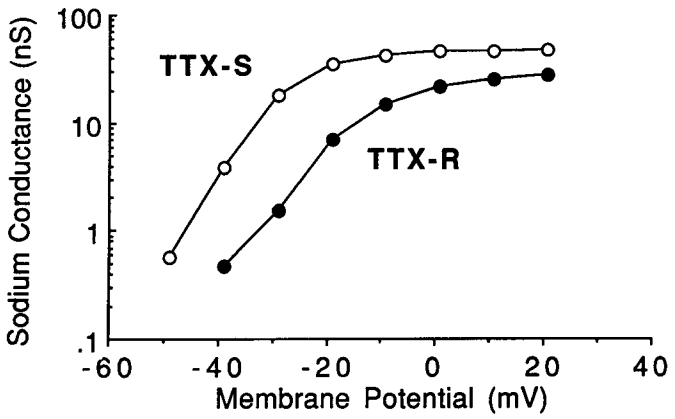


*Figure 4.* TTX-S and TTX-R current activation kinetics. Sodium conductances of two cells, one TTX-S and the other TTX-R, were calculated from peak current amplitudes and plotted as a function of membrane potential. For these cells, TTX-S and TTX-R values for 50% activation were −26.3 mV and −10.6 mV, respectively.

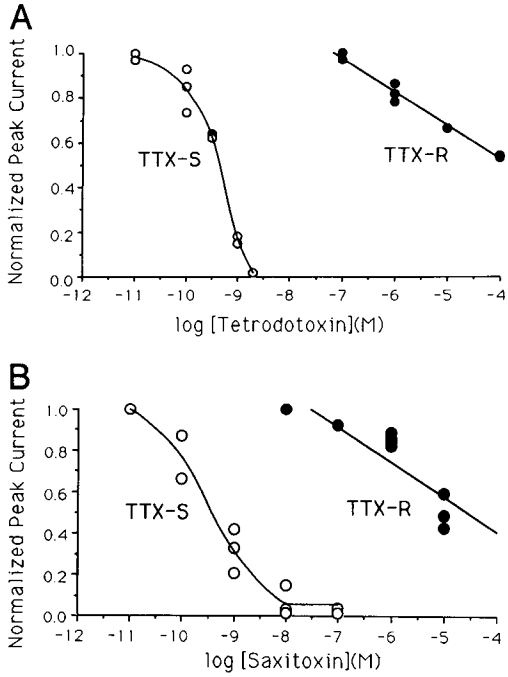


*Figure 5.* Dose–response relationships for TTX and STX block. Cells expressing solely TTX-S ($n = 3$) or TTX-R ($n = 3$) currents were exposed to increasing concentrations of TTX or STX and pulsed once per minute to +10 mV to determine peak current amplitude. Steady-state peak current amplitudes reached at each concentration were normalized to control toxin-free amplitudes and plotted against toxin concentration. *A*, TTX dose–response curve, with $K_d$ values of 0.3 nM (TTX-S) and 100 μM (TTX-R). *B*, STX dose–response curve, with $K_d$ values of 0.5 nM (TTX-S) and 10 μM (TTX-R).

In addition to resting block, lidocaine caused use-dependent block of sodium current during repetitive stimuli. From a holding potential of −80 mV, each cell studied was stimulated with 20 consecutive 40 msec pulses to +10 mV at 30–1000 msec intervals, corresponding to frequencies of 33.3–1 Hz. As indicated in Figure 6, *B* and *C*, this protocol was used in control solution (open symbols), as well as in the presence of 10 μM and 100 μM lidocaine (solid symbols) for TTX-S and TTX-R currents, respectively. The peak current amplitude for each pulse of a given frequency was normalized to that of the first pulse in the train, and is plotted against pulse number. For the TTX-S channels (Fig. 6*B*), lidocaine did not facilitate or augment the block at each stimulus frequency, indicating no marked use-dependent block. In the TTX-R channels, however, lidocaine significantly augmented the block at each stimulus frequency, indicating marked use-dependent block. Thus, while TTX-S current is more sensitive to resting lidocaine block, TTX-R current is more susceptible to use-dependent lidocaine block.

### *Effects of divalent cations*

The sensitivity of rat DRG TTX-R sodium channels to classical calcium channel blockers, such as certain divalent cations and D-600, has been previously reported (Kostyuk et al., 1981). In the present study, the effects of addition of 5 mM $Ca^{2+}$, 5 mM $Cd^{2+}$, and 50 μM $Pb^{2+}$ to the external solution on TTX-S and TTX-R currents were analyzed with the use of the current–voltage (*I–V*) protocol described earlier. Each of these divalent cations was added to the standard external solution, which contained 1.8 mM $Ca^{2+}$ and 1.0 mM $Mg^{2+}$.

The peak TTX-S current was reduced 22 ± 3.1% by addition of 5 mM $Ca^{2+}$ at −20 mV, 20.6 ± 2.2% by 50 μM $Pb^{2+}$ at −10 mV, and 30.1 ± 4.0% by 5 mM $Cd^{2+}$ at 0 mV relative to the control value at −15 mV ($n = 5$; Fig. 7*A*). The activation voltage for TTX-S channels was relatively unaffected by $Ca^{2+}$, but was shifted in the depolarizing direction by $Pb^{2+}$ and $Cd^{2+}$ (Fig. 7*A*). The shifts at the voltage at which conductance attained 50% of the maximal values were estimated to be +15.2 ± 1.5 mV ($n = 5$) for $Pb^{2+}$ and +25.5 ± 2.1 mV ($n = 5$) for $Cd^{2+}$. Conductance–voltage curves show a negligible decrease in maximal conductance by $Pb^{2+}$ (8.3 ± 2.8%; $n = 4$) and a more significant decrease by $Cd^{2+}$ (16.7 ± 3.9%; $n = 4$) (Fig. 8*A*). These effects of $Ca^{2+}$, $Pb^{2+}$, and $Cd^{2+}$ were reversible after washing for 1–2 min with test cation-free solution.

The peak TTX-R current was more sensitive to the actions of $Pb^{2+}$ and $Cd^{2+}$, and less sensitive to $Ca^{2+}$, than TTX-S current. The TTX-R current was reduced 8.2 ± 3% at −20 mV by addition of 5 mM $Ca^{2+}$, 70.4 ± 5.1% at +10 mV by 50 μM $Pb^{2+}$, 85.3 ± 4.2% at 0 mV by 5 mM $Cd^{2+}$, and 8.2 ± 3% at −20 mV by 5 mM $Ca^{2+}$, relative to the control peak amplitude at −15 mV ($n = 5$; Fig. 7*B*). The conductance–voltage curves, measured at potentials at which the conductance attained 50% of the maximal values, were shifted 25.3 ± 3.2 mV ($n = 4$) by $Pb^{2+}$ and 21.3 ± 3.1 mV ($n = 4$) by $Cd^{2+}$ (Fig. 8*B*). The maximal conductance was decreased 55.2 ± 1.9% ($n = 4$) by $Pb^{2+}$ and 69.3 ± 1.2% ($n = 4$) by $Cd^{2+}$ (Fig. 8*B*). These effects of $Pb^{2+}$, $Cd^{2+}$, and $Ca^{2+}$ were reversible after washing for 1–2 min with test cation-free solution.

## Discussion

STX and TTX are known to bind to a common site of TTX-S channels to cause a similar blocking effect, as illustrated by channel binding competition of STX with TTX (Ritchie and Rogart, 1977), and by electrophysiological experiments (Narahashi, 1974, 1988). As with various fish, molluscan, crustacean, amphibian, and mammalian preparations (Narahashi, 1974, 1988; Ritchie and Rogart, 1977), the rat DRG TTX-S sodium channel exhibited a nanomolar $K_d$ value for TTX block, as well as for STX block. In striking contrast to this value and the 1–6 μM $K_d$ value for TTX block of sodium channels in various cardiac muscle fibers (Brown et al., 1981; Catterall and Cop-

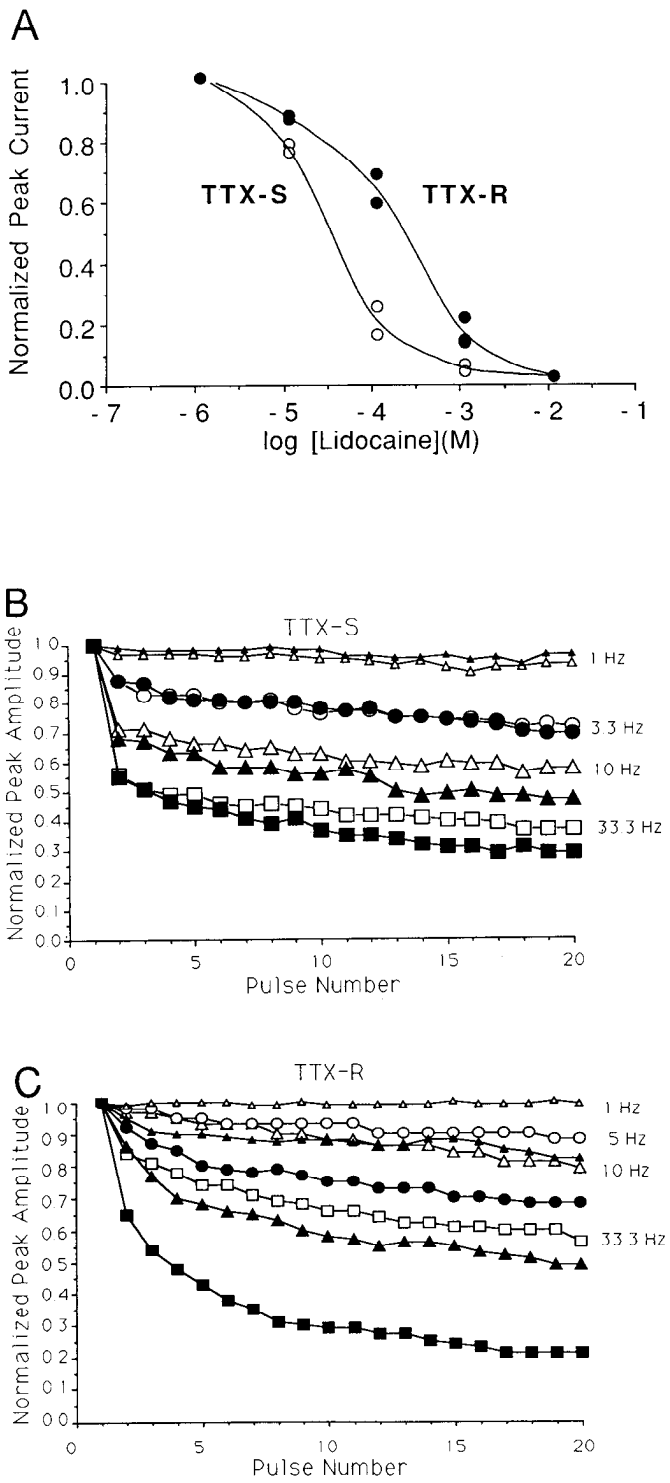


*Figure 6.* Dose–response relationships and use-dependent inhibition of the peak sodium current by lidocaine. *A,* Cells expressing solely TTX-S ($n = 3$) or TTX-R ($n = 3$) currents were exposed to increasing concentrations of lidocaine, with test pulses to +10 mV once every minute. $K_d$ values are 50 μM (TTX-S) and 200 μM (TTX-R). *B,* A cell expressing TTX-S current only was pulsed from a holding potential of −80 mV to +10 mV at frequencies ranging from 1 to 33.3 Hz. The current amplitudes were normalized to the initial peak current value and are plotted as a function of pulse number. *Open* and *solid symbols* represent data before and during application of 10 μM lidocaine, respectively. *Matching symbol shapes* reflect data at the same frequency. At higher frequencies (10–33.3 Hz), lidocaine suppressed the current slightly more than control, indicating a small degree of use-dependent block. *C,* A cell expressing only TTX-R current was similarly analyzed in the presence of 100 μM lidocaine, with a marked use-dependent lidocaine block observable at all test frequencies.

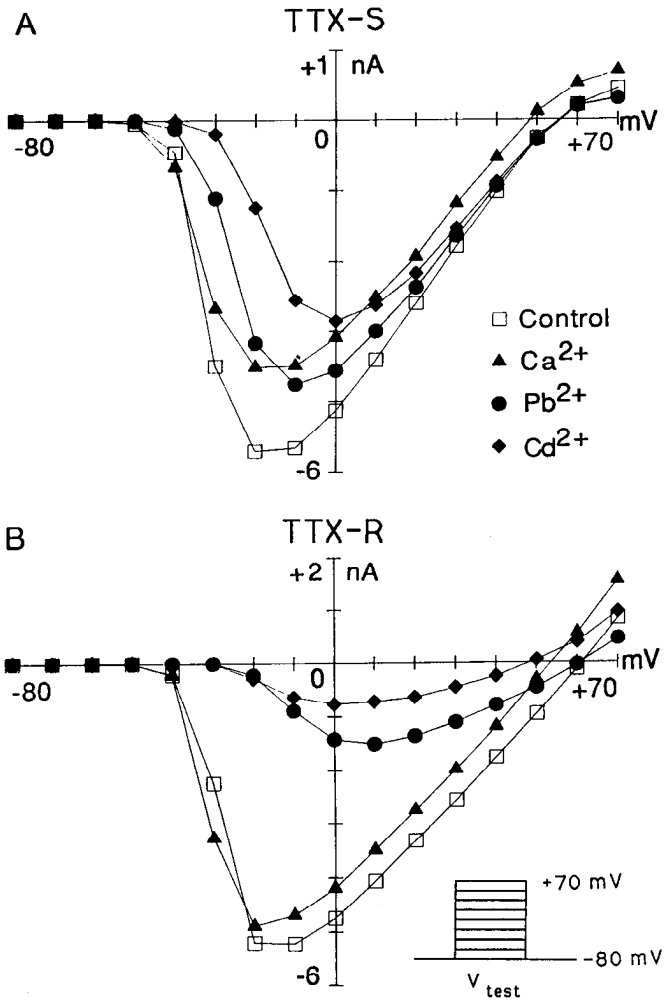


*Figure 7.* Effects of divalent cations on TTX-S and TTX-R channel current–voltage relationships. *A,* A cell expressing only TTX-S current was analyzed using the pulse protocol indicated in the *inset* in *B.* Current amplitudes in control and after addition of 5 mM $Ca^{2+}$, 50 μM $Pb^{2+}$ and 5 mM $Cd^{2+}$ are plotted as a function of membrane voltage. *B,* A cell expressing only TTX-R current was similarly analyzed. $Pb^{2+}$ and $Cd^{2+}$ both reduced the current amplitude and shifted the current–voltage curves in the depolarizing direction to a much greater extent in TTX-R current than in TTX-S current, whereas $Ca^{2+}$ had minimal effects.

persmith, 1981; Cohen et al., 1981), the rat TTX-R sodium channel exhibited a TTX $K_d$ value of ~100 μM for both TTX and STX. Thus, there may be structural differences in neurotoxin binding site between the neuronal TTX-R channel, the neuronal TTX-S channel, and cardiac muscle TTX-R channels.

TTX-R and STX-R channels have been reported in a wide variety of excitable tissues. An extensive study has shown that presence of these channels in various bivalve mollusk species (Twarog et al., 1972). Bullfrog sensory neurons exhibit an interesting TTX-R/STX-S profile (Jones, 1986), whereas bullfrog cardiac nerve and garter snake DRG neurons express channels that are both TTX-R and STX-R (Bowers, 1985; Campbell, 1988). Whereas previous research on the rat DRG TTX-R chan-

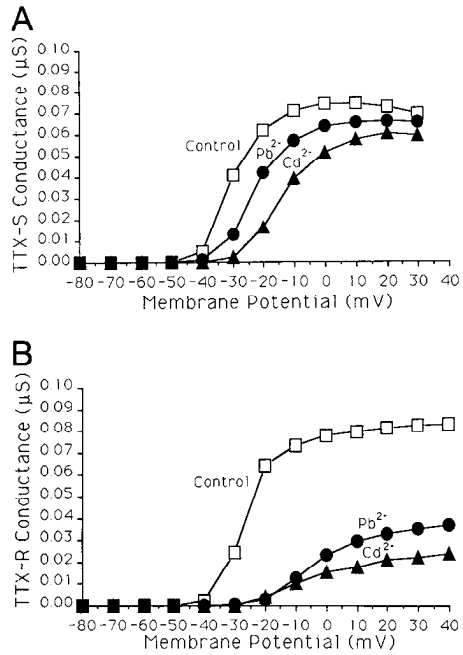


*Figure 8.* Effects of $Pb^{2+}$ and $Cd^{2+}$ on the conductance–voltage relationships of TTX-S and TTX-R channels. *A*, Peak current amplitudes recorded from a cell expressing TTX-S current were converted to conductances and plotted as a function of membrane potential. Both 50 μM $Pb^{2+}$ and 5 mM $Cd^{2+}$ shifted the conductance–voltage relationship in the depolarizing direction and had small suppressing effects on current amplitude. *B*, Analysis of TTX-R conductance–voltage relationship indicates a greater degree of depolarizing shift and current block by both 50 μM $Pb^{2+}$ and 5 mM $Cd^{2+}$.

nel has reported STX sensitivity (Barron et al., 1988), our present study indicates that this channel exhibits resistance to both TTX and STX.

The rat DRG TTX-S and TTX-R channels in the present study exhibited activation and inactivation kinetics similar to those reported by others in bullfrog and rat DRG neurons (Kostyuk et al., 1981; Guo and Strichartz, 1990; Omri and Meiri, 1990; Schwartz et al., 1990). These criteria were used recently to characterize sodium channel types in a study addressing the effect of NGF on neuronal channel expression (Omri and Meiri, 1990). DRG neurons were isolated from newborn rats and cultured for up to 30 hr in defined medium with or without NGF present. NGF was found to speed the development of TTX-S current expression relative to the NGF-free system. The DRG neurons used in our study were exposed to undetermined endogenous concentrations of NGF up until the time of animal death, with the youngest animals being 72 hr old. Whereas time frames and NGF exposures may differ in these studies, our TTX-R current exhibits activation and inactivation kinetics similar to those in NGF-free conditions, and our TTX-S current resembles a channel type reported to appear in the presence of NGF.

Cardiac TTX-R sodium channels (Cohen et al., 1981) and frog myelinated nerve TTX-S channels (Lonnendonker, 1989) exhibit use-dependent block by TTX. Use-dependent block by STX was demonstrated with TTX-S sodium channels of crayfish giant axons (Salgado et al., 1986). The presence or absence of TTX use-dependent block in rat DRG TTX-R sodium channels remains to be seen and is currently under investigation.

The effects of divalent cations on TTX-R and TTX-S currents reported previously (Kostyuk et al., 1981) were confirmed and analyzed further in the present study. The shifts of the conductance–voltage relationships in the direction of depolarization cannot be explained by the shielding phenomenon, in which the divalent cations interact with cell membrane surface negative charges, resulting in an increase in transmembrane potential, because an increase in $Ca^{2+}$ concentration to the same level as $Cd^{2+}$ did not cause a shift. In addition, the net concentration of sodium ions in the proximity of the sodium channel may be reduced due to competition with and repulsion of the divalent cations, but this factor also fails to explain the absence of effect of high $Ca^{2+}$ concentration. The reductions of TTX-R and TTX-S channel conductance are perhaps due to direct blocking actions of $Pb^{2+}$ and $Cd^{2+}$ on the channels.

Lidocaine has been shown to reduce sodium currents by interacting with the channel from the inside of the membrane (Frazier et al., 1970; Narahashi et al., 1970; Hille, 1977; Schwarz et al., 1977). Neuronal, skeletal, and cardiac muscle sodium channels each exhibit similar responses to tonic and use-dependent lidocaine block (Bean et al., 1983). The $K_d$ value for lidocaine block of the rat DRG TTX-R channel was similar to those reported for both the frog skeletal muscle TTX-S channel (Schwarz et al., 1977) and rabbit Purkinje neuron TTX-R channel (Bean et al., 1983). The rat DRG TTX-S channel, however, was more sensitive to block, in a manner comparable to that seen in the rat ventricular cell TTX-R channel (Lee et al., 1981).

The correlations of rat DRG TTX-R and TTX-S current expressions to cell size and animal age raise questions concerning the role of TTX-R channels in neuronal systems. With regard to cell size, cultured mammalian DRG neurons have been classified into two groups: (1) large neurons with short action potential duration, expressing TTX-S current; and (2) small neurons with long action potential duration, expressing TTX-R current. The former neurons are believed to give rise ultimately to the myelinated "A-α" or "A-β" fibers, whereas the latter become the slower "C" fibers (McLean et al., 1988). Regarding animal age and current expression, a question arises as to whether large DRG neurons expressing TTX-S current pass through a developmental stage as do smaller TTX-R cells. This type of process has been observed at the molecular level in perinatal rat skeletal muscle, in which the TTX-R channel mRNA isoform is gradually replaced by TTX-S channel mRNA over the first 3 postnatal weeks (Kallen et al., 1990). Evidence for a similar exchange in rat DRG neurons may be best illustrated by cells expressing both current types simultaneously in varying proportions (Kostyuk et al., 1981; McLean et al., 1988; Roy and Narahashi, 1990, 1991). Thus, TTX-R channels may have functional and temporal roles in the mature and developing mammalian CNS.

## References

Barron SE, Bennett PB, McLean MJ (1988) Effects of lidocaine and saxitoxin on the tetrodotoxin-resistant current of mammalian dorsal root ganglion neurons. Soc Neurosci Abstr 14:142.

Bean BP, Cohen CJ, Tsien RW (1983) Lidocaine block of cardiac sodium channels. J Gen Physiol 81:613–642.

Benzanilla F, Armstrong CM (1977) Inactivation of the sodium channel. I. Sodium current experiments. J Gen Physiol 70:549–566.

Bossu JL, Feltz A (1984) Patch-clamp study of the tetrodotoxin-resistant sodium current in group C sensory neurones. Neurosci Lett 51:241–246.

Bowers CW (1985) A cadmium-sensitive, tetrodotoxin-resistant sodium channel in bullfrog autonomic axons. Brain Res 340:143–147.

Brown AM, Lee KS, Powell T (1981) Voltage clamp and internal

perfusion of single rat heart muscle cells. J Physiol (Lond) 318:455–477.
Campbell DT (1988) Differential expression of Na channel subtypes in two populations of sensory neurons. Biophys J 53:15a.
Catterall WA, Coppersmith J (1981) Pharmacological properties of sodium channels in cultured rat hearts. Mol Pharmacol 20:533–542.
Cohen CJ, Bean BP, Colatsky TJ, Tsien RW (1981) Tetrodotoxin block of sodium channels in rabbit Purkinje fibers and interactions between toxin binding and channel gating. J Gen Physiol 78:383–411.
Frazier DT, Narahashi T, Yamada M (1970) The site of action and active form of local anesthetics. II. Experiments with quaternary compounds. J Pharmacol Exp Ther 171:45–51.
Guo X, Strichartz G (1990) Differential gating of TTX-sensitive and -resistant Na currents in bullfrog sensory neurons. Biophys J 57:107a.
Hamill OP, Marty A, Neher E, Sakmann B, Sigworth FJ (1981) Improved patch-clamp techniques for high-resolution current recording from cells and cell-free membrane patches. Pfluegers Arch 391:85–100.
Hille B (1975) The receptor for tetrodotoxin and saxitoxin, a structural hypothesis. Biophys J 15:615–619.
Hille B (1977) Local anesthetics: hydrophilic and hydrophobic pathways for the drug-receptor reaction. J Gen Physiol 69:497–515.
Ikeda SR, Schofield GG, Weight FF (1986) $Na^+$ and $Ca^{2+}$ currents of acutely isolated adult rat nodose ganglion cells. J Neurophysiol 55: 527–539.
Ikeda SR, Schofield GG (1987) Tetrodotoxin-resistant sodium current of rat nodose neurones: monovalent cation selectivity and divalent cation block. J Physiol (Lond) 389:255–270.
Jones SW (1986) Two sodium currents in dissociated bullfrog sympathetic neurons. Soc Neurosci Abstr 12:1512.
Kallen RG, Sheng ZH, Yang J, Chen L, Rogart RB, Barchi RL (1990) Primary structure and expression of a sodium channel characteristic of denervated and immature rat skeletal muscle. Neuron 4:233–242.
Kostyuk PG, Veselovsky NS, Tsyndrenko AY (1981) Ionic currents in the somatic membrane of rat dorsal root ganglion neurons—I. Sodium currents. Neuroscience 6:2423–2430.
Lee KS, Hume JR, Giles W, Brown AM (1981) Sodium current depression by lidocaine and quinidine in isolated ventricular cells. Nature 291:325–327.
Lonnendonker U (1989) Use-dependent block of sodium channels in frog myelinated nerve by tetrodotoxin and saxitoxin at negative holding potentials. Biochim Biophys Acta 985:153–160.
Marty A, Neher E (1983) Tight-seal whole-cell recording. In: Single channel recording (Sakmann B, Neher E, eds), pp 107–122. New York: Plenum.
Matsuda Y, Yoshida S, Yonezawa T (1978) Tetrodotoxin sensitivity and Ca component of action potentials of mouse dorsal root ganglion cells cultured *in vitro*. Brain Res 154:69–82.
Matteson DR, Armstrong C (1984) Na and Ca channels in a transformed line of anterior pituitary cells. J Gen Physiol 83:371–394.
McLean MJ, Bennett PB, Thomas RM (1988) Subtypes of dorsal root ganglion neurons based on different inward currents as measured by whole-cell voltage clamp. Mol Cell Biochem 80:95–107.
Narahashi T (1974) Chemicals as tools in the study of excitable membranes. Physiol Rev 54:813–889.
Narahashi T (1988) Mechanisms of tetrodotoxin and saxitoxin action. In: Handbook of natural toxins (Tu A, ed), pp 185–210. New York: Dekker.
Narahashi T, Frazier DT, Yamada M (1970) The site of action and active form of local anesthetics. I. Theory and pH experiments with tertiary compounds. J Pharmacol Exp Ther 171:32–44.
Omri G, Meiri H (1990) Characterization of sodium currents in mammalian sensory neurons cultured in serum-free defined medium with and without nerve growth factor. J Membr Biol 115:13–29.
Ritchie JM, Rogart RB (1977) The binding of STX and TTX to excitable tissue. Rev Physiol Biochem Pharmacol 79:1–50.
Rogart RB, Cribbs LL, Muglia LK, Kephart DD, Kaiser MW (1989) Molecular cloning of a putative tetrodotoxin-resistant rat heart Na channel isoform. Proc Natl Acad Sci USA 86:8170–8174.
Roy ML, Narahashi T (1990) Differential properties of tetrodotoxin-sensitive and tetrodotoxin-resistant sodium channels in rat dorsal root ganglion neurons. Soc Neurosci Abstr 16:181.
Roy ML, Narahashi T (1991) Effects of saxitoxin, divalent cations and lidocaine on tetrodotoxin-sensitive and tetrodotoxin-resistant sodium channels in rat dorsal root ganglion neurons. Biophys J 59:263a.
Salgado VL, Yeh JZ, Narahashi T (1986) Use- and voltage-dependent block of the sodium channel by saxitoxin. Ann NY Acad Sci 479:84–95.
Schwartz A, Palti Y, Meiri H (1990) Structural and developmental differences between three types of Na channels in dorsal root ganglion cells of newborn rats. J Membr Biol 116:117–128.
Schwarz W, Paladi PT, Hille B (1977) Local anesthetics: effects of pH on use-dependent block of sodium channels in frog muscle. Biophys J 20:343–368.
Twarog BM, Hidaka T, Yamaguchi H (1972) Resistance to tetrodotoxin and saxitoxin in nerves of bivalve molluscs. Toxicon 10:273–278.
Yoshida S, Matsuda Y, Samejima A (1978) Tetrodotoxin-resistant sodium and calcium components of action potentials in dorsal root ganglion cells of the adult mouse. J Neurophysiol 41:1096–1106.